



HAL
open science

Contact resistivity of Al/Ti ohmic contacts on p-type ion implanted 4H and 6H-SiC

Roberta Nipoti, Francesco Moscatelli, Andrea Scorzoni, Antonella Poggi, Gian Carlo Cardinali, Mihai Lazar, Christophe Raynaud, Dominique Planson, Marie-Laure Locatelli, Jean-Pierre Chante

► To cite this version:

Roberta Nipoti, Francesco Moscatelli, Andrea Scorzoni, Antonella Poggi, Gian Carlo Cardinali, et al.. Contact resistivity of Al/Ti ohmic contacts on p-type ion implanted 4H and 6H-SiC. 2002 MRS Fall Meeting, Dec 2002, Boston, United States. 10.1557/PROC-742-K6.2 . hal-02485106

HAL Id: hal-02485106

<https://hal.science/hal-02485106>

Submitted on 19 Feb 2020

HAL is a multi-disciplinary open access archive for the deposit and dissemination of scientific research documents, whether they are published or not. The documents may come from teaching and research institutions in France or abroad, or from public or private research centers.

L'archive ouverte pluridisciplinaire **HAL**, est destinée au dépôt et à la diffusion de documents scientifiques de niveau recherche, publiés ou non, émanant des établissements d'enseignement et de recherche français ou étrangers, des laboratoires publics ou privés.

Contact resistivity of Al/Ti ohmic contacts on p-type ion implanted 4H- and 6H-SiC.

Roberta Nipoti, Francesco Moscatelli¹, Andrea Scorzoni¹, Antonella Poggi, Gian Carlo Cardinali, Mihai Lazar², Christophe Raynaud², Dominique Planson², Marie-Laure Locatelli² and Jean-Pierre Chante²

CNR- IMM Sezione di Bologna, via Gobetti 101, 40129 Bologna

¹Dipartimento d'Ingegneria Elettronica e dell'Informazione, Università di Perugia, via G.

Duranti 93, 06125 Perugia

²CEGELY (UMR CNRS n°5005), Bât. Leonard de Vinci, INSA de Lyon, 20, Av. A. Einstein, F-69621, Villeurbanne Cdx France

ABSTRACT

Al-Ti alloys with 72 wt% Al were employed for the realisation of ohmic contacts on $4 \times 10^{19} \text{ cm}^{-3}$ p-type ion implanted 4H- and 6H-SiC samples. Contact resistivity characterisations by TLM measurements were done at wafer level in the temperature range 28-290°C. Analysis of the TLM measurements took into account current crowding at the metal pads. More than half of the evaluated contact resistivity reached the minimum value detectable by the used TLM devices, that was slightly higher than $1 \times 10^{-6} \Omega \text{ cm}^2$. Above this limit value, contact resistivity decreased for increasing temperature and was spread over a few decades. The maximum contact resistivity at 28°C was $2 \times 10^{-4} \Omega \text{ cm}^2$, which changed to $5 \times 10^{-6} \Omega \text{ cm}^2$ at 290°C. The thermal behaviour of these TLM structures featured thermionic-field emission conduction.

INTRODUCTION

Al-Ti alloys have been subjects of several electrical, chemical and physical investigations aimed at making ohmic contacts on p-type SiC [1]. The alloy with the 70 wt% Al was found to give the more reproducible specific contact resistivity ρ_c after vacuum annealing at 1000°C for 2 min. These ρ_c values ranged from $1.5 \times 10^{-4} \Omega \text{ cm}^2$ to $9.5 \times 10^{-6} \Omega \text{ cm}^2$ for doping concentration ranging from $7 \times 10^{18} \text{ cm}^{-3}$ to $1.3 \times 10^{19} \text{ cm}^{-3}$, respectively, independently of the 4H- or 6H-SiC polytype [2]. Moreover, the lowest ρ_c values were found to be independent of the alloy ratio [2, 3]. These studies featured as grown SiC epilayer, mesa etching, Al-Ti sintered targets of the desired weight ratio and lift off technology to define the metal pattern for the ρ_c evaluation.

The purpose of this work was to transfer the 70 wt% Al recipe [2] to p-type ion implanted 4H- and 6H-SiC specimens. Due to technological constraints some steps were modified. In particular, single element targets were used and the layer thickness ratio was chosen so to obtain the desired Al/Ti weight ratio. The metal patterns were defined by chemical etching. Different gases in the annealing ambient were studied, namely high purity Ar and vacuum.

The Transmission Line Method (TLM) was used to evaluate the ρ_c of these Al-Ti alloyed contacts. In particular, the resistance measurements on TLM structures were analysed accounting for two-dimensional (2D) and three-dimensional (3D) current flow.

EXPERIMENTAL

<0001> 8° off-axis 4H-SiC and <0001> on-axis 6H-SiC, n-type wafers supplied by CREE were used for this study. Almost box shaped doping profiles were made at the sample surface via

multiple energy Al⁺ implantation and high temperature thermal annealing. The substrate temperature during implantation was varied in the range 27-300°C from sample to sample. The implanted wafers were annealed one by one at 1700°C in an inductively heated J.I.P.ELECTM furnace equipped with a glassy carbon crucible covered by a SiC disk. The annealing gas was high purity Ar at a partial pressure just above the atmospheric one. Secondary Ion Mass Spectrometry showed the as implanted and annealed doping profiles were the same, while Hall effect measurements at room temperature showed hole density values corresponding to a complete electrical activation of the implanted Al. The p-type implanted layers had doping concentration and thickness equal to $4 \times 10^{19} \text{ cm}^{-3}$ and 1.35 μm for the 6H-SiC wafer, $4.5 \times 10^{19} \text{ cm}^{-3}$ and 0.38 μm for the 4H-SiC one.

<0001> 3.5° off-axis 6H-SiC wafer by CREE with a 2 μm thick $1 \times 10^{19} \text{ cm}^{-3}$ p-type epilayer on an n-type substrate was also used for comparison.

The TLM metal patterns were realised by the following recipe. The samples were cleaned consecutively in boiling trichlorethylene, acetone and isopropyl alcohol. This degreasing in organic solvent was followed by the next surface cleaning recipe H₂SO₄:H₂O₂ (1:1) for 5min, deionised water for 3min, HF:H₂O=1:10 for 60s, deionised water for 3min. At the end of this cleaning process, the substrates were dried with N₂ gas. Before loading in the vacuum chamber for metal deposition, the samples were dipped in HF: H₂O = 1:1 for 30s and dried with N₂ gas. First Ti (80 nm) and then Al (350 nm) were deposited by sputtering. The chosen thicknesses correspond to 72 wt% Al. Photolithography process and subsequent metal etching were employed to define the metal patterns. Post deposition annealing was done at 1000°C for 2 min and different annealing ambients were tested: high purity Ar gas and vacuum (10⁻⁶ torr).

TLM structures featured two mask levels in the case of the implanted wafers and one mask level in the case of the epilayer specimen. In fact, in the former case doped strips, below the metal pads, were defined by mesa etching or selective ion implantation, while in the epilayer case the conductive paths were not confined. In the implanted specimens Van der Pauw (VdP) devices, for a direct extraction of the sheet resistance R_{sh} of the implanted layers, were defined too. Different sets of TLM devices were used. On the 6H-SiC wafer, 341 μm wide doped strips with 296 μm wide and 132 μm long metal pads with increasing distances between consecutive pads of 18-27-37-57-108 μm were realised (TLM1). On the 4H-SiC wafer, the TLM structures were 150 μm wide doped strips with 94 μm wide and 94 μm long metal contacts with increasing distances between consecutive pads of 9-18.5-28-37.5-47-57 μm (TLM2). While on the epilayer, TLM metal patterns equal to those used for the 4H-SiC specimen were produced. The given figures were measured after contact alloying and by using an optical microscope, with measurement error equal to $\pm 0.5 \mu\text{m}$.

Current-voltage (I-V) measurements on the TLM and VdP devices were performed as a function of the temperature in the range 28-290°C using a computer controlled parametric characterisation system. This was equipped with a Micromanipulator MM6620 semiautomatic probe station, a Temptronic TP315B hot chuck, a Keithley K707 switching matrix (equipped with 7072 and 7174 semiconductor cards) and a Keithley K90 I-V measuring system, composed by a Keithley K2361 synchronisation controller and four Keithley K238 source measure units. An average of ten TLM and ten VdP devices homogeneously distributed over a 35 mm or 50 mm wafers were typically measured per sample type.

ρ_c was evaluated by resistance measurements on TLM structures. These TLM structures were included in masks designed for the realisation of given SiC devices and it was found their geometry with respect to the sheet resistance of the implanted layers could not be treated by the

usual one-dimensional (1D) approach. Neither the measurements of non-confined TLM structures could be treated by a 1D approach. Thus, lateral current crowding at the metal pads was taken into account under a 2D approximation. As shown in ref. [4-6] this can be done under the assumptions that the sheet resistance of the doped layer between and that below the pads are equal, and that the transfer length $\sqrt{\rho_c / R_{sh}}$ is at least three times, or more, the doped strip depth. Taking into account the transfer length is ρ_c dependent the check of the latter condition was done once the 2D simulated ρ_c was obtained. Should not this condition be fulfilled, a correction factor for ρ_c would be computed following the indication given in ref. [7].

The sheet resistance of the strip layer was a variable parameter in the 2D code and at the same time it could be directly measured by means of VdP devices. The comparison between these computed and measured values was used as reliability check for the code outputs.

RESULTS

Fig. 1(a,c) shows the total resistance R_{total} data versus pad distance L and their simulation under 1D and 2D approximations. The search for optimal ρ_c and R_{sh} values was done through a 2D best fit of the R_{total} versus L . The TLM measured resistances and simulations shown in this picture belong to the 6H-SiC ion implanted wafer, but their trend was representative of all those here studied. In particular, the 2D approximation always accounted better than the 1D approach for the curvature of the experimental data. The 2D simulations always compute R_{total} values at $L = 0$ lower than those computed by the 1D model. The differences between the intercepts at $L = 0$ were always approximately independent of ρ_c but dependent on and almost constant for given TLM device geometry and doped layer R_{sh} . This is evidenced in Fig. 1(b,d) that is an enlarged view of Fig. 1(a,c) next to $L = 0$. Such differences amounted at $(25 \pm 5) \Omega$ and $(196 \pm 5) \Omega$ for the TLM1 and TLM2 pattern type, respectively.

Fig. 2 shows the R_{sh} values extracted from the 2D model for the doped strips of the TLM structures (TLM R_{sh}) versus the corresponding ones obtained from the VdP measurements (VdP R_{sh}). The VdP devices had square shape with a side parallel to the wafer flat, while the TLM doped strip were aligned both parallel and orthogonal to the wafer flat. The 4H- and 6H-SiC implanted samples at the minimum and maximum measurement temperatures were chosen as representative of all the samples here studied. The evident spread of the

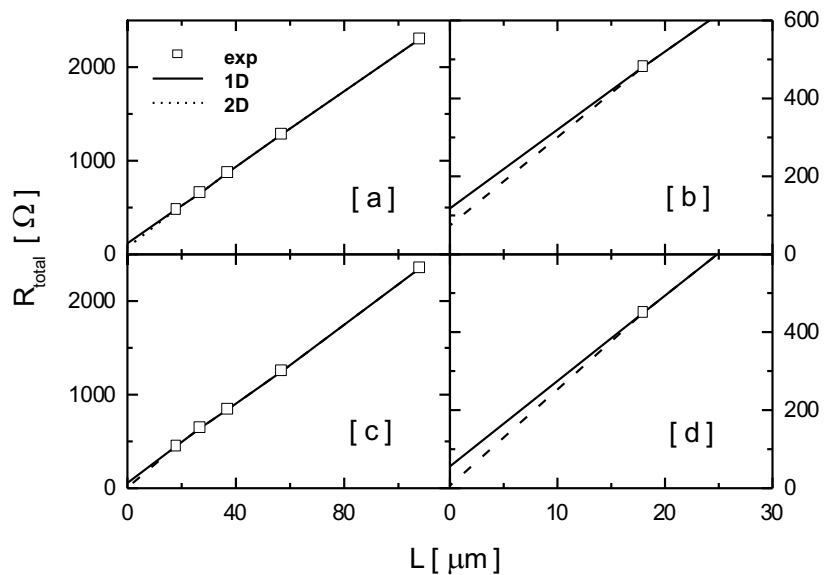


Figure 1. Two meaningful cases from the 6H-SiC ion implanted wafer have been chosen to show the trend of the experimental (exp) and simulated (1D, 2D) data. [a] and [c] show the whole measurement range, [b] and [d] are enlarged views close to $L = 0$.

VdP R_{sh} values for each measurement temperature is a consequence of the temperature gradient across the wafer diameter during the ion implantation annealing process as discussed in ref. [8]. Simulated and measured values are linearly related through a factor equal to (1.06 ± 0.01) .

Taking into account the ρ_c evaluated by the 2D model and the corresponding transfer length with respect to the thickness of the doped layer, the 2D ρ_c values had to be transformed into the equivalent 3D ones by applying correction factors in the range 1.2 and 3 [7]. Generally, lower were the 2D ρ_c values higher were the correction factors. Moreover, it was found that the used TLM geometry did not allow us to extract ρ_c values lower than approximately $1 \times 10^{-6} \Omega\text{cm}^2$.

The equivalent 3D ρ_c values are plotted in Fig. 3 versus measurement temperature. Fig. 3(a,b) shows the ρ_c for the not confined TLM devices, i.e. for the $1 \times 10^{19} \text{ cm}^{-3}$ 6H-SiC epilayer. Fig. 3(a) corresponds to high purity Ar annealing ambient, while Fig. 3(b) to vacuum ambient. The ρ_c values for the ion implanted 4H-SiC and 6H-SiC specimens, i.e. $4 \times 10^{19} \text{ cm}^{-3}$ doping density, are shown in Fig. 3(c) and Fig. 3(d), respectively. All the ρ_c values below the minimum resolution of the method were set equal to $1 \times 10^{-7} \Omega\text{cm}^2$. These last ρ_c values were not meaningful but indicated a very good ohmic performance. The error bars are shown only for one data set per picture and account for the minimisation process between simulated and experimental results.

Finally, the yield of the ρ_c values shown in Fig. 3(c,d) is plotted in Fig. 4 for different measurement temperatures.

DISCUSSION

The linearity of the Fig. 2 plot is an indirect proof of the reliability of the results provided by the simulation code, i.e. of the estimated ρ_c values. The fact the proportionality factor differs

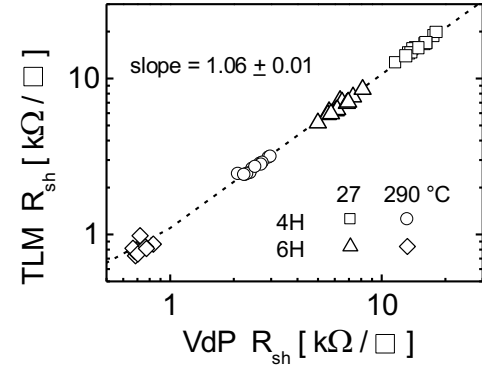
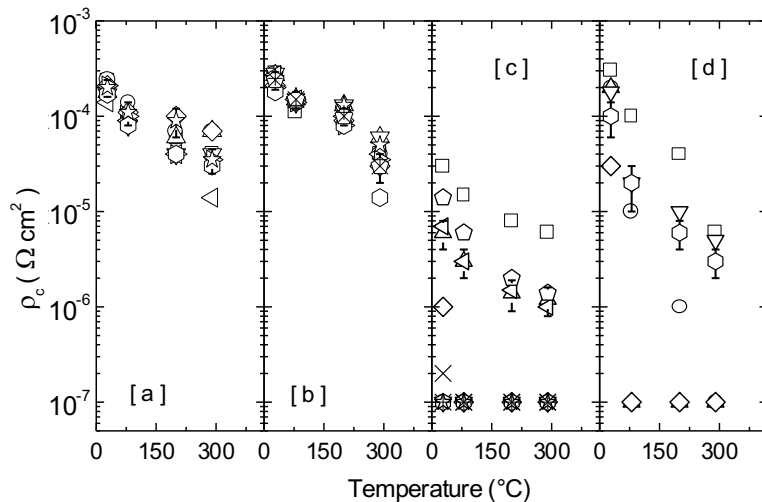


Figure 2. Sheet resistances of the TLM structures extracted from the 2D model versus the corresponding values obtained from the VdP measurements.

Figure 3. Contact resistivity versus temperature for the not confined TLM patterns alloyed in Ar [a] or vacuum ambient [b], and for the confined TLM devices of the ion implanted 4H-SiC [c] and 6H-SiC [d] wafers. All the evaluated ρ_c data are shown, while the error bars corresponding to the minimisation procedure between simulated and measured TLM measurements values are shown for only one data set in each sub-figure.

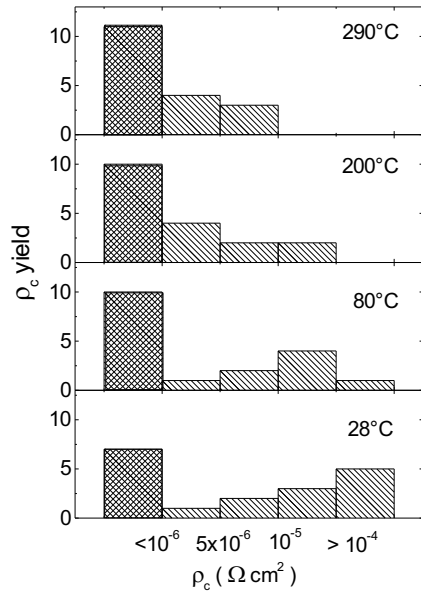


Figure 4. Yield of the ohmic contact process for the implanted wafers with respect to the contact resistivity mapped at wafer level. 4H- and 6H-SiC results were joined.

attributed to local differences in the electrical activation of the implanted doping species [8]. In fact, when the estimated ρ_c values above the minimum resolution of the method are compared with the literature data [1-3] the plot of Fig. 5 is obtained. Looking at this figure, we can remark the data of the implanted specimens fall in a region where ρ_c is expected to be high sensitive to small variation of the doping concentration.

A further remark can be done about Fig. 5. The ρ_c evaluated at the highest temperature has a better agreement with the trend of the published values for contacts with an equivalent weight percent of Al. It looks like the barrier height for conduction was higher in the ion implanted samples than in the epitaxial ones. In general, the thermal behaviour of these ρ_c featured thermionic-field emission conduction at the contact interface. Nevertheless, even at room temperature, many ρ_c values were below the minimum detectable limit (see Fig.4), i.e. they were better than the published values. In this case we might speculate about reasons to justify a lower barrier height for conduction in the implanted specimens with respect to the

from 1 within the errors may be due to almost unavoidable non-ideal effects in the VdP geometry and/or a consequence of the approximations used for the 2D simulation of the resistance measurements of the TLM structures. In such a case the correction factors applied to the 2D ρ_c might be different than the applied ones. Nevertheless it can be remarked that these correction factors were so low that the corrected ρ_c remained of the same order of magnitude and had the same trend versus temperature as the 2D ρ_c .

A typical problem of the Al/Ti alloyed contact annealed in Ar is the oxidation of the pad top surface [9]. Such an oxide is hard to remove and makes difficult the wafer level characterisation of the devices. Therefore, post annealing in vacuum is generally preferred. The results plotted in Fig. 3(a) and in Fig. 3(b), show that, once the probing problem was solved, the ρ_c performances for annealing in high purity Ar or in vacuum are equivalent. In the light of this result, the ρ_c values of all the samples here presented were analysed independently of the annealing ambient, as done in Fig.4.

The comparison between Fig. 3(a,b) and Fig. 3(c,d) evidences the spread of the ρ_c values is negligible in the case of the epitaxial wafer, while it is as large as a few decades for the ion implanted specimens. Such a difference might be

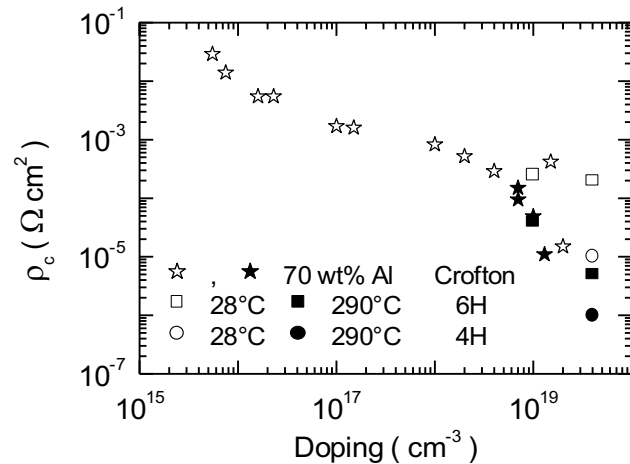


Figure 5. Contact resistivity versus p-type doping: comparison between literature (stars) and this work data at room temperature (open square and dots) and 290°C (full square and dots). The literature data referring to the 70 wt% Al are evidenced as full stars.

epitaxial substrates. We think such non-homogeneous behaviour of the contacts at wafer level might be understood looking for correlation among electrical performances of different devices at different temperatures. This work is in progress.

Finally, the yields shown in Fig. 4 suggest the technology for the realisation of ohmic contacts to SiC is so mature that the Kelvin resistor method [4] could be introduced for the evaluation of ρ_c on ion implanted SiC, both 4H and 6H.

CONCLUSION

This work demonstrates the technology of Al/Ti alloyed contacts on p-type ion implanted 4H- or 6H-SiC can give quite low values of ρ_c . In fact, in spite of the large spread of the results, the ρ_c values were always lower than $2 \times 10^{-4} \Omega\text{cm}^2$ for a medium/high doping concentration of the implanted layers, i.e. $4 \times 10^{19} \text{cm}^{-3}$. Moreover, a non-negligible yield of values below $1 \times 10^{-6} \Omega\text{cm}^2$ was found. The results for 4H- and 6H-SiC were similar.

Moreover, this study demonstrates the analysis of non-ideal TLM test structures can be faced and solved by taking into account current crowding, thus reaching a better knowledge about the contact performance.

Work partially funded by the Italian Contracts CNR-MADESS-II and ASI/CNR(1/R/073/01). The clean room staff of CNR-IMM Sezione di Bologna is acknowledged for TLM metal pattern realisation.

REFERENCES

1. J. Crofton, L. Beyer, J. R. Williams, E. D. Luckowski, S. E. Mohny, J. M. DeLucca, "Titanium and aluminum-titanium ohmic contacts to p-type SiC," *Solid-State Electron.*, **41**, 1725 (1997).
2. J. Crofton, S. E. Mohny, J. R. Williams, T. Isaacs-Smith, "Finding the optimum Al-Ti alloy composition for use as an ohmic contact to p-type SiC," *Solid-State Electron*, **46**, 109 (2002).
3. J. Crofton, P. A. Barnes, J. R. Williams, J. Edmond, "Contact resistance measurements on p-type 6H-SiC," *Appl. Phys. Lett.*, **62**, 384 (1993).
4. A. Scorzoni and M. Finetti, "Metal /semiconductor contact resistivity and its determination from contact resistance measurements", *Material Science Report*, **3** no. 2 (1988).
5. Scorzoni, M. Finetti, G. Soncini and I. Suni, "Ohmic contact resistance evaluation in silicon planar structures: application to the CoSi_2/n^+ interface," *Alta Freq* **61**, 341 (1987).
6. Finetti, A. Scorzoni and G. Soncini, "Lateral current crowding effects on contact resistance Measurements in four terminal resistor test patterns," *IEEE Electron Device Letters*, **EDL-5**, no. 12, 524 (1984).
7. B. Schuldt, "An exact derivation of contact resistance to planar devices", *Solid-State Electronics*, **21**, 715 (1978).
8. M. Lazar, C. Raynaud, D. Planson, M.L. Locatelli, K. Isoird, L. Ottaviani, J.P. Chante, R. Nipoti, A. Poggi, G. Cardinali, "A comparative study of high-temperature aluminium post-implantation annealing in 6H- and 4H-SiC, non uniform temperature effects", *Material Science Forum* **389-393**, 827 (2002).
9. F. Moscatelli, A. Scorzoni, A. Poggi, G. C. Cardinali and R. Nipoti "Al/Ti Ohmic Contacts to p-type Ion Implanted 6H-SiC: Mono- and Two-dimensional Analysis of the TLM Data" Accepted for publication in *Material Science Forum* 2003